# Influence of $Nb_2O_5$ Polymorphism on Adsorption Process

**Vinícius S. Santana[1]; Rodrigo De Paula[1]**

*[1] UFRB – Universidade Federal do Recôncavo da Bahia, Amargosa, Bahia, Brasil.*
**email: viniciussantana524@gmail.com*

**Keywords**: niobium oxide, polymorphs, adsorption, x-ray diffraction

## 1. Introduction

Environmental pollution is a global issue that affects various ecosystems and human health. Among the many aspects of pollution, the contamination of watercourses is particularly concerning due to its importance for life and the sustainability of natural resources. To combat water pollution, conventional treatments such as filtration, coagulation, sedimentation, and the use of chemical reagents are widely used, which remove contaminants and ensure the quality of drinking water (Papagiannaki, 2022).

However, these traditional methods have limitations, especially in treating emerging pollutants. These contaminants, primarily originating from industrial and domestic activities, are increasingly present in everyday life and pose challenges to conventional treatments, as they can be toxic even at low concentrations (Otavo-Loaiza, 2019). In Brazil, concern about emerging contaminants has increased significantly (Farto, 2021).

The development of new materials is one of the fundamental pillars for technological advancement in various sectors, including environmental protection (Lopes, 2015). In this regard, innovative materials, especially those based on metal oxides, have gained prominence. Among them, niobium pentoxide ($Nb_2O_5$) stands out for its unique characteristics, showing promise for various processes, such as Advanced Oxidation Processes (AOPs) used in the degradation of emerging contaminants (Gallo, 2016). $Nb_2O_5$, a transition metal oxide, presents several polymorphs, each with distinct properties related to thermal treatment (Morais, 2016). Some of these polymorphs demonstrate chemical stability, but their crystallinity also depends on the level of purity, the precursor used, and the heating rate (Rosário, 2002). This oxide can exist in different crystalline forms: amorphous, monoclinic, orthorhombic, and hexagonal—with atomic arrangements that directly influence its physical and chemical properties, such as adsorption capacity, which will be discussed in this work.

In adsorption tests, which are essential for understanding the interaction between solid surfaces and adsorbed molecules, the polymorphism of $Nb_2O_5$ can significantly influence the material's performance as an adsorbent (Ben Hammouda, 2021). Adsorption is crucial for removing contaminants in aqueous solutions, and the efficiency of this process depends on factors such as surface area, porosity, and the presence of active sites on the material's surface. Some characterizations, which we will discuss here, are critical to optimizing these tests. Different polymorphic forms of $Nb_2O_5$ may exhibit variations in surface area and pore distribution, affecting the material's ability to adsorb specific molecules (Silva, 2022). Thus, understanding how polymorphism affects these characteristics is essential for optimizing the use of $Nb_2O_5$ in environmental and industrial applications.

The study of $Nb_2O_5$ polymorphism and its influence on adsorption tests is relevant due to the need to develop more efficient and sustainable materials for environmental applications. Brazil stands out in this context as the largest producer of this oxide, with 89% of the world's exploitable reserves and as the largest exporter of this element (Brazil, 2024). With the increase in water contamination by recalcitrant organic compounds, such as pesticides, pharmaceuticals, and other emerging pollutants, it is crucial to find effective and economically viable alternatives for effluent treatment.

Therefore, investigating the influence of $Nb_2O_5$ polymorphism on adsorption tests not only expands knowledge about the properties of this material but also opens new possibilities for its application in strategic areas, such as environmental protection and the chemical industry. Understanding how different crystalline forms affect the performance of $Nb_2O_5$ in adsorption processes makes it possible to develop more specialized and higher-performing materials, contributing to technological advancement and sustainability across various sectors.

In this context, the objective of this study was to perform structural, elemental, and surface characterization of six $Nb_2O_5$ samples, kindly provided by the Companhia Brasileira de Metalurgia e Mineração (CBMM). At this point, we will not discuss photocatalysis; instead, we will present a review of characterization techniques and an adsorption study.

## 2. Methods and materials

The work was carried out following the guidelines of the research group in Organic Physical Chemistry, with the first part focused on characterizations, as the synthesis was not our responsibility but rather that of our partner, CBMM (Companhia Brasileira de Metalurgia e Mineração).

### 2.1 X-ray diffraction (XRD)

The crystalline structure measurements of the samples were performed using a Rigaku Ultima IV diffractometer, powder method, with Cu Kα radiation (λ = 1,154118 nm), Scanning from 2° to 75° at 2°/min, 40 kV, and 30 mA. The simulated pattern of the diffractograms was obtained based on the crystalline structure, in collaboration with CBMM, which provided a detailed report.

### 2.2 Wavelength Dispersive X-ray Fluorescence Spectrometrya (WD-FRX)

The chemical composition of the different polymorphs was obtained by wavelength-dispersive X-ray fluorescence spectrometry (WD-XRF) performed on an S8 Tiger Bruker with a vacuum atmosphere, a rhodium (Rh) source, a Si(Li) semiconductor detector, and a 10 mm collimator, with tube voltages of 50 kV (Ti-U) and 15 kV (Na-Sc), and operating energies of up to 40 and 4.4 keV, respectively.

### 2.3 Point of Zero Charge (PZC)

The point of zero charge (PZC) of the $Nb_2O_5$ samples was determined using the solid addition method, following the guidelines of the works by Lima (2018) and Galvão (2022). To conduct the study, 50 mL of solution with different initial pH conditions (pHi), ranging from 1 to 13, were added to seven beakers. To adjust the pHi, hydrochloric acid (HCl) and sodium hydroxide (NaOH) solutions at 1.0 mol/L were used. pH adjustments were made with a pH

meter from MS TECNOPON, model mPA-210. Subsequently, in each beaker with adjusted pHi, 50 mg of the Nb2O5 samples were added, and the solution was maintained on a magnetic stirrer from IKA, model C-MAG HS 7, with stirring at 1500 rpm for twenty-four hours at room temperature in a closed system. After this period, the samples were filtered, and the final pH (pHf) of each filtrate was measured. Based on the pHf values, a plot of pH variation ($\Delta pH = pH_i - pH_f$) versus pHi was created, and the point of intersection, where $\Delta pH = 0$, corresponds to the point of zero charge (Galvão, 2022).

### 2.4 Adsorption assays

For these assays, a variety of materials and glassware were used, including volumetric flasks, Erlenmeyer flasks, beakers, filters, automatic micropipettes, Pasteur pipettes, spatulas, magnetic stir bars, clamps, and a universal support. Also utilized were a semi-analytical balance (brand: Marte, model: AY220), a magnetic stirrer (brand: IKA, model: C-MAG HS 7), pH meters (brand: MSTECNOPON, model: mPA-210; brand: Digimed, model: DM-23-DC), and a UV-VIS spectrophotometer (brand: Global Trade Technology, model: UV-5100).

#### 2.4.1 Construction of the calibration curve

To obtain the calibration curve, a stock solution of the yellow tartrazine dye with a concentration of 5.343 mg/L (Solution A) was initially prepared, and from this solution, a more diluted solution with a concentration of 50 mg/L (Solution B) was prepared. Different systems with concentrations ranging from 9.98 to 50 mg/L were prepared. After preparation, 500 µL of HCl was added to each Erlenmeyer flask with the respective concentrations to maintain an acidic load. The absorbance of each sample was measured using a spectrophotometer. For the readings, nine aliquots of 3000 µL of Solution B of the yellow tartrazine dye were added to a glass cuvette. For each aliquot added, the absorbance value was measured with the spectrophotometer at the maximum absorption wavelength ($\lambda$ max = 427 nm), using distilled water as the baseline. Through the nine different concentration points with their respective absorbance values, a linear relationship between absorbance measurement and solution concentration was established.

### 2.5 Adsorption studies

#### 2.5.1 Adsorption isotherms

Adsorption isotherm studies with the $Nb_2O_5$ polymorphs were conducted for nine systems at a temperature of 25°C ± (2°C) and under stirring at 1500 rpm for 24 hours. The dye used in the adsorption experiments was yellow tartrazine. ($C_{16}H_9N_4Na_3O_9S_2$) With a molar mass of 534.30 g/mol, nine solutions of the dye with different concentrations were prepared from the diluted solution with a concentration of 50 mg/L. Subsequently, 50 mg of Nb2O5 was added to each of these solutions. To determine the amount of dye adsorbed from the solution, the spectrophotometric method was employed, with measurements taken after a defined adsorption period.

Upon reaching adsorption equilibrium, the final solute concentration in the equilibrium solution (Ce, in mg/L) and the adsorption capacity of the adsorbent (qe, in milligrams of adsorbate per gram of adsorbent) are determined. To calculate the values of qe, a mass balance

must be performed, where the amount of adsorbate on the adsorbent should equal the amount of adsorbate removed from the solution. Mathematically, this can be expressed as follows:

$$qe = \frac{(C_O - C_e) * V}{m} \quad (1)$$

*where: qe: adsorption capacity (mg/g), Co: initial concentration of the adsorbate (mg/L)*

*Ce: equilibrium concentration of the adsorbate (mg/L), V: volume of the solution (L)*

*m: mass of the adsorbent (g)"*

After obtaining the data, to establish a more suitable correspondence for the equilibrium curves of yellow tartrazine adsorbed by different Nb2O5 polymorphs, four adsorption isotherm models were used: Langmuir, Freundlich, Temkin, and Redlich-Peterson (Foo, 2010). The Langmuir theory proposed to explain adsorption on a uniform, simple, infinite, and non-porous surface. This model is based on the hypothesis that adsorbed molecules move freely across the adsorbent surface (Langmuir, 1918). As more molecules are adsorbed, they are evenly distributed, forming a monolayer that covers the entire surface. Thus, at equilibrium, a saturation point is reached where no further adsorption occurs. This model is useful for understanding adsorption under ideal conditions of uniform surfaces and non-interactive adsorbed molecules (Nascimento et al., 2014, p.27).

The Langmuir isotherm expression is represented by the equation: 2:

$$qe = \frac{q_{max} * K_L * C_e}{1 + K_L * C_e} \quad (2)$$

*where: qe: adsorption capacity (mg/g), qmax: maximum adsorption capacity (mg/g), $K_L$: adsorbate/adsorbent interaction constant (L/mg), Ce: equilibrium concentration of the adsorbate (mg/L).*

The Freundlich isotherm is used for systems with heterogeneous surfaces, that is, adsorption in multilayers with interaction between adsorbate molecules, where an exponential distribution is applied to characterize the various types of adsorption sites, which have different adsorption energies (Massarani, 1997; Nascimento et al., 2014, p.27).

The Freundlich isotherm expression is represented by Equation 3:

$$qe = K_F * (Ce)^{1/n} \quad (3)$$

*where: qe: amount of adsorbed solute (mg/g), Ce: equilibrium concentration of the adsorbate (mg/L), 1/n: constant related to the heterogeneity of the surface, $K_F$: Freundlich adsorption capacity constant*

The Temkin isotherm incorporates a factor that describes the interactions between the adsorbate and the adsorbent. This two-parameter equation considers the interactions between the adsorbent and the adsorbate, as well as the uniform distribution of binding energies (Foo, 2010). Additionally, it is not suitable for extremely low or high concentrations. The equation is based on the heat of adsorption of the process, which decreases linearly with the increase in

adsorbent surface coverage (Aharoni, 1977; Ungarish, 1977, cited in Nascimento et al., 2014, p. 39). The expression for the Temkin isotherm is given by Equation 4:

$$qe = \frac{RT}{b} * \ln(a_T * Ce) \quad (4)$$

*where: qe: amount of solute adsorbed at equilibrium (mg/g), Ce: concentration of the adsorbate in solution at equilibrium (mg/L), T: Temperature (K), b: Temkin constant related to the heat of sorption, R: universal gas constant (8.314 J/mol·K), $K_T$: binding equilibrium constant (L/mg)*

The empirical Redlich-Peterson equation can be applied to adsorption processes over a wide range of concentrations. It is a hybrid isotherm that combines characteristics of both the Langmuir and Freundlich isotherms (Foo, 2010). With respect to this variable, the model features an exponential function in the denominator and a linear dependence in the numerator, making it applicable to both homogeneous and heterogeneous systems (Ng, 2002; Gimbert, 2008).

The isotherm equation has three parameters and is given by Equation 5:

$$qe = \frac{K_{RP}Ce}{1 + a_{RP}Ce^{\beta}} \quad (5)$$

*where: $K_{RP}$ and aRP are the Redlich-Peterson constants (L/mg), $\beta$ is the exponent that ranges from 0 to 1*

The empirical Redlich-Peterson equation combines characteristics of the Langmuir and Freundlich models. In the limit, the model approaches the Freundlich isotherm at high concentrations, when the exponent β approaches zero, and it aligns with the Langmuir ideal condition at low concentrations, when the values of β are close to one (Jossens, 1978; Foo, 2010; Nascimento et al., 2014, p.42).

## 3. Results and Discussion

### 3.1 X-ray diffraction (XRD)

X-ray diffraction (XRD) is a fundamental technique for analyzing the crystallinity of materials, used to structurally characterize crystalline solids. This method is based on the arrangement of atoms in crystal planes, separated by distances comparable to the wavelengths of X-rays used in diffraction. When an X-ray beam strikes a crystal, it interacts with its atoms, resulting in the phenomenon of diffraction (Skoog, Holler, and Crouch, 2007).

Figure 1 compiles the diffractograms of the samples provided by CBMM, which was responsible for the synthesis. The Nb2O5 samples were named 4381, 8070, 8071, 9375, 9376, and 9377. The experimental results indicated the absence of a defined crystal structure for sample 4381, while the other polymorphs exhibit defined crystallinity; additionally, some are mixtures of phases.

**Figure 1**: X-ray Diffraction Spectra of the Nb2O5 Polymorphs

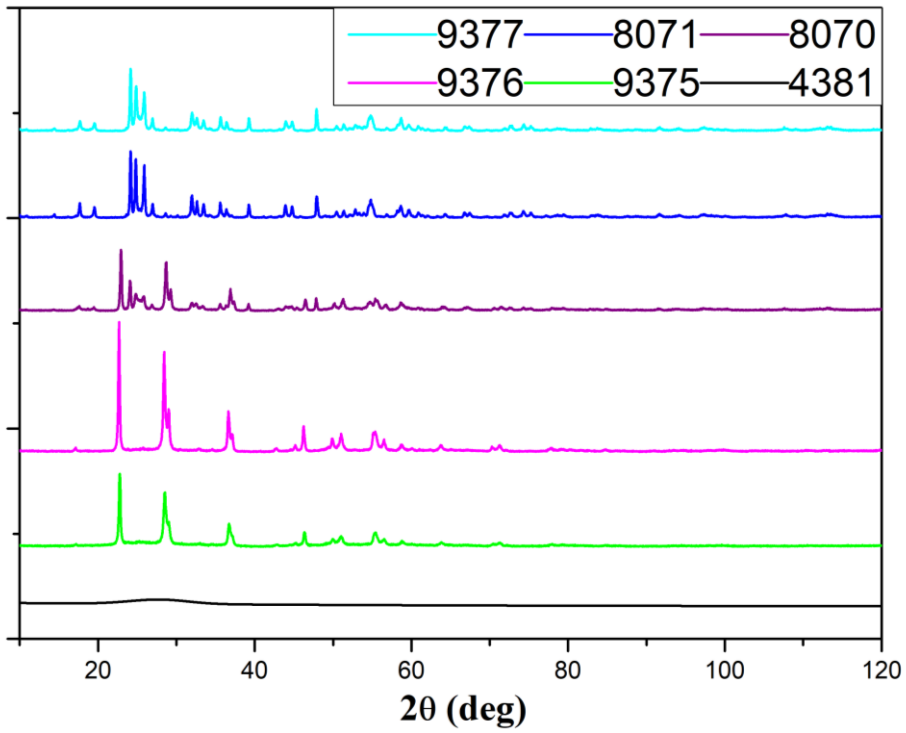


**Fonte:** (author, 2023)

Due to the absence of characteristic peaks in the material named 4381, it was classified as amorphous. However, it is important to note that thermal treatment is a determining factor in forming a crystalline structure. Although it does not solely depend on this factor, crystallinity is also related to the material's purity level, the precursor used, and the heating rate (Rosário, 2002; Morais, 2016).

According to data from CBMM and Silva (2022), sample 4381 was prepared at a calcination temperature of 400°C. This temperature provided insufficient energy for the formation of crystal structure, which is why it does not exhibit a defined crystalline phase. Studies by Carvalho (2018), Lacerda (2020), Gallo (2016), and Morais (2016) reported that the commercial oxide 4381, produced by CBMM, is an amorphous solid. Thus, the result described here for oxide 4381 is consistent with the reports from these authors. Samples 9375, 9376, and 8070 were subjected to thermal treatment and calcination at temperatures of 600°C, 600°C, and 900°C, respectively, according to information provided by CBMM. Temperatures above 500°C reveal some of the niobium phases. Although these samples were prepared at these temperatures, they exhibited a mixture of phases because they were calcined outside the ideal range to achieve a single phase.

Studies by Falk (2017) and Silva (2022) reported the possibility of phase coexistence when the material is calcined at temperatures not specific to the required conditions. Thus, the $Nb_2O_5$ polymorph 8070 can be classified as a material with T and M phases (Falk, 2017; Silva, 2022). Following this reasoning, polymorphs 9375 and 9376, which were prepared at different calcination temperatures, present a mixture of T and TT phases, with the only difference between them being the percentage of these phases.

Samples 8071 and 9377, which were subjected to a calcination temperature of 1200°C, correspond to the monoclinic phase, which is the most stable phase for $Nb_2O_5$. According to the literature, the monoclinic phase, referred to as phase H (from 'Hoch', meaning 'high' in German), is the thermodynamically most stable crystalline phase and is obtained in processes involving calcination temperatures above 1000°C (Falk, 2017; Silva, 2022). According to Silva (2022), sample 8071 was compared with an XRD database from consulted sources. The diffractograms were superimposable, indicating that it is a material with a defined and pure crystalline phase, confirming its stability as a polymorph. Based on this statement, sample 9377, which was calcined at the same temperature as 8071, presents the same diffractogram. The difference between the polymorphs is minimal, being only 0.8%. This information was provided by CBMM. Therefore, in addition to the cited works, the XRD graphs are consistent with Jia (2020) for the TT, T, and H phases.

Table 1 presents, in a compiled form, the information extracted from the X-ray diffraction analysis of the polymorphs studied in this work. It is worth noting that the information provided by CBMM is not reported in the literature and is, initially, the exclusive property of the company. However, after successive exchanges of messages, the values described here were shared as a contribution to the preparation of this work.

**Table 1:** Percentage of the crystalline phase and calcination temperature of each Nb2O5 polymorph

| Polymorph | Calcination temperature (°C) | Crystalline phase, % |
|---|---|---|
| 9377 | 1200 | H - 100% |
| 8071 | 1200 | H – 99.2% |
| 8070 | 900 | M - (64.7%) e T - (35.3%) |
| 9376 | 600 | T - (93.8%) e TT - (6.2%) |
| 9375 | 600 | T - (75.7%) e TT - (24.3%) |
| 4381 | 450 | — |

### 3.2 Wavelength Dispersive X-ray Fluorescence Spectrometrya (WD-FRX)

Of the six samples received from CBMM, one exhibited a yellowish coloration, distinct from the others, which were white, the typical color of oxides. This difference raised concern and led to elemental analysis by WD-FRX. Table 2 presents the elemental composition of the six studied polymorphs, as this variation in coloration may impact adsorption and photocatalytic tests.

**Table 2:** Elemental percentage of each crystalline phase of the Nb2O5 polymorphs

| | Polymorphs | | | | | |
|---|---|---|---|---|---|---|
| **Analyte** | **4381** | **9375** | **9376** | **8070** | **8071** | **9377** |
| Nb2O5 | 99.57% | 96.78% | 99.19% | 99.44% | 99.17% | 99.49% |
| $Ta_2O_5$ | - | 18 ppm | 0.44% | 0.50% | 0.44% | 0.44% |
| $SO_3$ | - | 2,70% | 39 ppm | - | - | - |
| $SiO_2$ | - | 0.15% | 0.10% | - | 0.13% | 0.03% |
| $Al_2O_3$ | - | 0.07% | 0.02% | - | - | - |
| $MoO_3$ | - | 0.06% | - | - | - | - |
| $K_2O$ | - | 0.06% | 0.01% | - | 0.08% | - |

| | | | | | | |
|---|---|---|---|---|---|---|
| $Fe_2O_3$ | 0.03% | 0.04% | 0.03% | 0.03% | 0.07% | 0.02% |
| CaO | - | 0.04% | 0.06% | - | 0.04% | - |
| $TiO_2$ | 0.38% | 0.03% | 0.03% | - | 0.06% | 0.02% |
| Ag | - | 0.03% | 0.03% | - | - | - |
| Cl | - | 0.02% | 0.08% | 0.03% | - | - |
| $Ga_2O_3$ | - | 54 ppm | - | - | - | - |
| NiO | - | 53 ppm | 51 ppm | 64 ppm | 49 ppm | 43 ppm |
| ZnO | - | - | 32 ppm | - | 37 ppm | - |
| $Cr_2O_3$ | - | - | - | - | 0.01% | - |
| CuO | 0.02% | - | - | - | - | |

### 3.3 Point of Zero Charge (PZC)

According to the chosen methodology, tests were conducted to determine the Point of Zero Charge (PZC) for $Nb_2O_5$ polymorphs prepared at different calcination temperatures. The Point of Zero Charge (PZC or $pH_{PZC}$) is a fundamental description of a material's surface. The $pH_{PZC}$ is the pH at which the sum of the surface charge on a solid is zero (Lima, 2018; Galvão, 2022). This technique allows for identifying how the surface responds to variations in acidity or alkalinity of the medium.

To understand the differences between the PZC values of $Nb_2O_5$ polymorphs, X-ray diffraction (XRD) proved to be an excellent allied technique, as diffractograms made it possible to identify the crystalline phase of each polymorph. The surface of the polymorph is generally formed by $OH^-$ groups that are either protonated or deprotonated depending on the acidity or alkalinity of the reacting solution (Silva, 2018 apud Silva, 2022).

When the pH is higher than the $pH_{PZC}$, the surface is negatively charged, and the reaction medium is basic; the $OH^-$ groups are deprotonated, which favors the adsorption of cations. Conversely, when the pH is lower than the $pH_{PZC}$, the surface is positively charged in an acidic medium; the $OH^-$ groups are protonated, favoring the adsorption of anions (Silva, 2022; Nascimento et al., 2014).

Depending on the type of substance intended for adsorption on an oxide surface, pH adjustment is necessary to achieve greater adsorption. Therefore, surface study is important because, in adsorption processes, it is beneficial for the adsorbate and adsorbent charges to be opposite to maximize electrostatic interaction between them (Nascimento et al., 2014 apud Galvão, 2022).

For instance, the study model of this work involves organic substrates with a negative charge, as it concerns an azo dye. Thus, the reaction medium should have a pH below the $pH_{PZC}$. As observed in Table 3, the pH values corresponding to the PZC of each analyzed oxide differ, along with their respective average deviations.

**Table 3:** Values Obtained for the $pH_{PZC}$ of Each $Nb_2O_5$ Polymorph Studied Through the Solid Addition Method

| **Polymorphs** | **$pH_{PZC}$** | **Standard deviation** |
|---|---|---|
| 9377 | 5,57 | ±0,60 |

| | | |
|---|---|---|
| 8071 | 7,56 | ±0,74 |
| 8070 | 4,46 | ±1,17 |
| 9376 | 3,98 | ±1,61 |
| 9375 | 3,47 | ±1,22 |
| 4381 | 3,10 | ±1,24 |

The estimation of the point of zero charge ($pH_{PZC}$) is a property that helps to understand the pH value at which the surface charge distribution of a solid material ceases to exist, meaning when the sum of the surface charges is zero. However, it is important to note that there are different methods for estimating this parameter, and each method may provide distinct values, even for the same type of material (Cristano et al., 2011).

The behavior of samples 8070, 9375, and 9376, which reflect their phase mixtures, shows multiple inflection points and thus generates more than one $pH_{PZC}$ value. Literature values for oxides calcined at low temperatures are generally low, ranging from 3.0 to 4.94. For instance, Domingues et al. (2019) found a $pH_{PZC}$ value of 3.90 for hydrated niobium oxide ($Nb_2O_5.nH_2O$ - 4381). Kosmulski (2009) reported a value of 4.10, while Bolzon and Prado (2011) obtained 4.94.

A detailed analysis of the characteristics of the surfaces of the six studied polymorphs revealed that the adopted procedure is effective for understanding the behavior of the surface concerning the acidity of the medium. This parameter is especially important for applications as a photocatalyst because the photocatalytic process involves the adsorption of a substrate onto the metal oxide. Understanding the surface charge distribution of the oxide is crucial for enhancing adsorption, particularly when the nature of the substrate, whether neutral or ionic, is known.

### 3.4 Adsorption assays

#### 3.4.1 Construction of the calibration curve

According to the literature, the maximum absorbance peak of the yellow tartrazine dye is at $\lambda max$ = 426 nm. To verify if the wavelength found experimentally matches the literature value, a scan was performed using a spectrophotometer. It was observed that the dye to be used in the experiments had a maximum absorbance peak at 427 nm, a value very close to that reported in the literature. Once the maximum absorbance peak was identified, measurements of the absorbances of the dye solutions, with concentrations ranging from 9.98 to 50 mg/L, were taken at this specific wavelength. These data allowed for the construction of the analytical curves presented in figure 2, which shows the spectrum of the yellow tartrazine dye in the range of 300 to 800 nm, as well as the analytical curve fitted to the linear equation at 427 nm, with a coefficient of determination $R^2$ = 0.9992.

**Figure 2**: Left: Absorption spectrum of the yellow tartrazine dye, Right: Calibration curve of the yellow tartrazine dye

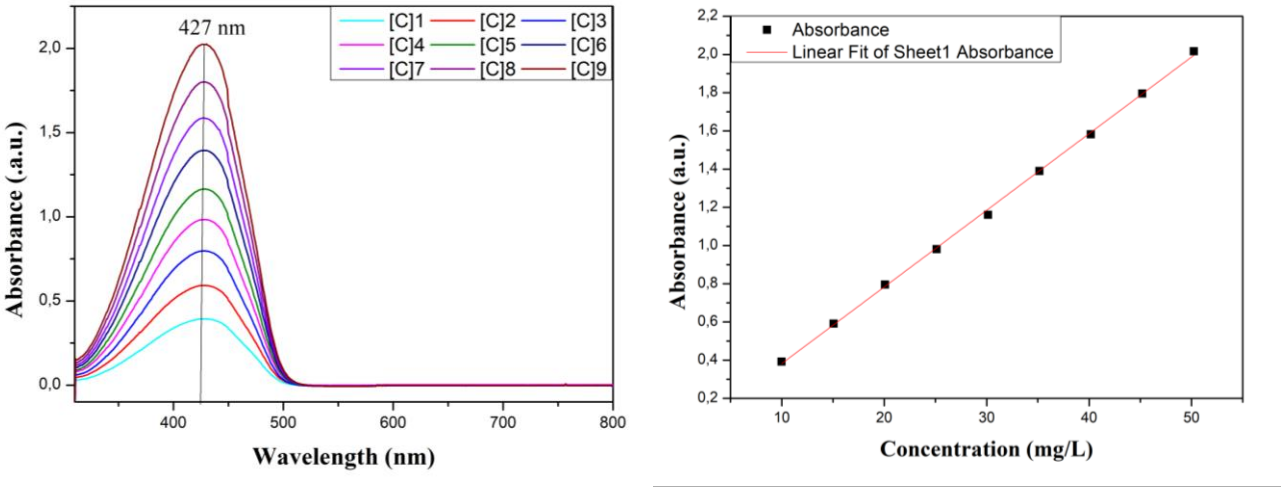


**Fonte**: author, 2024

### 3.5 Adsorption studies

#### 3.5.1 Adsorption isotherms

One way to characterize the surface of solids is through adsorption. In this study, tests were conducted involving six polymorphs of $Nb_2O_5$ using the yellow tartrazine dye as a model substrate. When the adsorbate comes into contact with the adsorbent, the molecules migrate from the aqueous phase to the surface of the adsorbent until the solute concentration in the liquid phase (Ce) remains constant. At this point, the system reaches equilibrium, and the adsorptive capacity of the adsorbent (qe) is determined (Nascimento et al., 2014). From the absorbance measurements and the calibration curve, the equilibrium concentration and the parameter qe, defined as the amount of dye adsorbed by the $Nb_2O_5$ polymorphs, were calculated. Using the experimental equilibrium results, a graph was constructed relating the amount of adsorbed dye (qe) to the equilibrium concentration in the liquid phase (Ce).

For the dye studied, the temperature was maintained constant at 25°C ± 2°C. After preparation, 500 µL of HCl were added to each Erlenmeyer flask, with the respective concentrations, to maintain an acidic load, as the dye adsorption occurs in an acidic medium due to the anionic nature of the substrate. To establish the best fit for the equilibrium curves and estimate the parameters of the isotherms, the Langmuir, Freundlich, Temkin, and Redlich-Peterson models were adjusted to the experimental data (Foo, 2010). Table 4 presents the isotherm parameters and the quality of the fit for the adsorption of yellow tartrazine on the different $Nb_2O_5$ polymorphs.

**Table 4:** Parameters of Isotherms for the Adsorption of Tartrazine Dye on Different $Nb_2O_5$ Polymorphs

| **Isotherm model** | **Sample** | | | | | |
|---|---|---|---|---|---|---|
| ***Langmuir*** | **4381** | **9375** | **9376** | **8070** | **8071** | **9377** |
| *Qm* ($mg*g^{-1}$) | 30.90 | 10.53 | 8.83 | 7.70 | 11.60 | 1.15 |
| $K_L$ | 0.187 | 0.07 | 0.05 | 0.49 | 0.03 | 0.44 |

| | | | | | | |
|---|---|---|---|---|---|---|
| $R_L$ | 0.15 | 0.66 | 0.89 | 0.49 | 0.89 | 0.67 |
| $R^2$ | 0.96 | 0.83 | 0.60 | -0.16 | 0.65 | -0.12 |
| ***Freundlich*** | | | | | | |
| $K_F\ (mg*g^{-1}(L*mg^{-1})^{1/n})$ | 7.52 | 1.69 | 1,11 | 4.67 | 0.79 | 0.91 |
| *1/n* | 0.39 | 0.41 | 0,46 | 0.12 | 0.57 | 0.04 |
| $R^2$ | 0.93 | 0.73 | 0,70 | -0.14 | 0.66 | -0.14 |
| ***Temkin*** | | | | | | |
| $K_T\ (L*mg^{-1})$ | 1.72 | 0.52 | 0.61 | 170 | 0.35 | $5.52*10^{-7}$ |
| *RT/b* | 6.92 | 2,60 | 1.88 | 0.84 | 2.35 | 0.05 |
| $R^2$ | 0.96 | 0,81 | 0.70 | -0.14 | 0.60 | -0.14 |
| ***Redlich-Peterson*** | | | | | | |
| $K_{RP}(L*mg^{-1})$ | 6.06 | 0,40 | 12,621 | $4.48*10^{-7}$ | 0.23 | 0.07 |
| $a_{RP}\ (L*mg^{-1})^{1/\beta}$ | 0.22 | $9*10^{-5}$ | 11,396 | $9.96*10^{-6}$ | $2.97*10^{-7}$ | $3.61*10^{-6}$ |
| $\beta$ | 0.97 | 2,58 | 0.53 | 0.87 | 6.30 | 3.53 |
| $R^2$ | 0.95 | 0,95 | 0.64 | -0.54 | 0.65 | -0.15 |

The $R^2$ values presented in Table 3 shows that, among the four adsorption isotherm models studied, the one that best fit the experimental equilibrium data was the model for the amorphous polymorph, represented by sample 4381, considered as $Nb_2O_5 * nH_2O$. This sample, calcined at low temperatures, exhibited higher adsorption capacity compared to the other studied polymorphs. This indicates that the dye adsorption occurred at homogeneous and specific sites of $Nb_2O_5 * nH_2O - 4381$ and was of a chemical nature. Therefore, the Langmuir, Freundlich, Temkin, and Redlich-Peterson isotherm models can be used to represent the experimental equilibrium data for the dye adsorption $Nb_2O_5 * nH_2O - 4381$, as the $R^2$ value was close to 1. Additionally, the $R_L$ values showed that the adsorption process was favorable for all the polymorphs. However, in samples where this value was close to 1, it was observed that the adsorption process was linear, indicating a proportional relationship between concentration and the other polymorphs. In Rodrigues' work (2008), which used the same hydrated polymorph studied here for phosphate ion ($PO4^{3-}$) adsorption, the Langmuir and Freundlich parameters mentioned in the previous table were higher, due to the specific characteristics of the adsorbate studied. In contrast, the other polymorphs with defined crystallinity did not show good adsorption capacity, possibly due to their crystalline stability. However, sample 9375, which has a phase mixture including the hexagonal phase (one of the first to show crystallinity for the $Nb_2O_5$ polymorph), could be quantified through XRD. The models that fit this sample were Langmuir and Redlich-Peterson, as the $R^2$ value was close to 1. In Taher's work (2021), the T phase of the $Nb_2O_5$ polymorph was used for batch adsorption tests with methylene blue dye, comparing it with the amorphous phase of the same polymorph. Taher observed that the T phase was superior to the amorphous phase. However, in this study, although the T phase did not show superiority over the amorphous phase, the graph obtained is in agreement with Taher's (2021) results for the T phase for samples 8070, 9375, and 9376. Although samples 8071 and 9377 present monoclinic phases, they should have similar adsorption characteristics. However, as described in the XRF analysis, the presence of different

oxides in sample 8071 resulted in higher adsorption capacity compared to sample 9377, as evidenced by the studied adsorption models.

## Conclusion

The results demonstrate that the adsorption capacity of $Nb_2O_5$ varies depending on its polymorph, with the Langmuir and Freundlich models providing the best fits. This highlights the influence of the adsorbent's structure on the effectiveness of tartrazine dye adsorption. Specifically, the amorphous polymorph ($Nb_2O_5 * nH_2O - 4381$) exhibited the highest adsorption capacity, indicating that dye adsorption occurs on homogeneous and specific sites of this material with a chemical nature. Polymorphs with defined crystallinity, such as the T phase and monoclinic phases (8071 and 9377), showed variable adsorption capacities, with the presence of different phases and impurities affecting their performances. The analysis of the results confirms that the pH of the medium and the material's purity significantly impact adsorption efficiency. Comparison with previous studies, such as those by Taher (2021), also highlights that, although some samples exhibited adsorption characteristics similar to the T phase, adsorption capacity is influenced by factors such as the presence of different crystalline phases and impurities in the polymorphs. Therefore, selecting the appropriate polymorph and understanding its structural properties are crucial for optimizing dye adsorption and other substrate applications in practical settings.

## Agradecimentos

We are grateful to UFRB for the financial support through the scholarship. We are also thankful to CBMM/Araxá MG for providing all the materials studied in this work, as well as for conducting some XRD analyses. Our thanks extend to Dr. Prof. Dr. Yuji N. Watanabe (UFRB/CFP) and Dr. Gerônimo L. Lima (UFRB/CFP) for their valuable contributions, as well as to the personnel at LABCAT (UFBA).

## Referências

BEN HAMMOUDA, Samia et al. Recent advances in developing cellulosic sorbent materials for oil spill cleanup: A state-of-the-art review. *Journal of Cleaner Production*, v. 311, p. 127630, 2021.

BOLZON, L. B.; PRADO, A. G. S. Effect of protonation and deprotonation on surface charge density of Nb2O5. *Journal Of Thermal Analysis And Calorimetry*, [S.L.], v. 106, n. 2, p. 427-430.

CARVALHO, K. T. G. Síntese e modificação de óxidos de nióbio para uso como catalisadores em reações de oxidação: estudos por cálculos teóricos e evidências. 2009.

CRISTIANO, E. et al. A comparison of point of zero charge measurement methodology. *Clays and Clay Minerals*, v. 59, n. 2, p. 107-115, 2011.

FALK, G. da S. O. Nanoparticulados e estudo de suas propriedades fotocatalíticas. 2017.

FARTO, Cindy Deina et al. Contaminantes emergentes no Brasil na década 2010-2019–parte I: ocorrência em diversos ambientes aquáticos. *Revista de Gestão de Água da América Latina*, v. 18, n. 2021, 2021.

FERNANDO, Santos Domingues et al. Photocatalytic degradation of real textile wastewater using carbon black-Nb2O5 composite catalyst under UV/Vis irradiation. *Environmental Technology (United Kingdom)*, v. 42, n. 15, 2021.

FOO, K. Y.; HAMEED, B. H. Insights into the modeling of adsorption isotherm systems. *Chemical Engineering Journal*, v. 156, n. 1, p. 2-10, 2010.

GALLO, Inara Fernanda Lage. Preparação e caracterização de fotocatalisadores heterogêneos de titânio e nióbio e avaliação do potencial de fotodegradação. 2016. Tese (Doutorado). Universidade de São Paulo.
GALVÃO, Lourdes Oliveira. O uso da biomassa residual do cacau como uma proposta de oficina temática para o ensino de equilíbrio químico. 2022.

GIMBERT, F. et al. Adsorption isotherm models for dye removal by cationized starch-based material in a single component system: error analysis. *Journal of Hazardous Materials*, v. 157, p. 34-46, 2008.

JIA, Yongfang et al. *The Journal of Physical Chemistry C*, 2020.

JOSSENS, L. et al. Thermodynamics of multi-solute adsorption from dilute aqueous solutions. *Chemical Engineering Science*, v. 33, p. 1097-1106, 1978.

KOSMULSKI, M. Surface Charging and Points of Zero Charge. Boca Raton: CRC Press, 2009.

LACERDA, Elenice Hass Caetano. Modificação de argila bentonita com pentóxido de nióbio para remediação de efluentes têxteis. 2020. Tese (Doutorado em Química). Universidade Estadual de Ponta Grossa, Ponta Grossa, 2020.

LANGMUIR, Irving. *Journal of the American Chemical Society*, v. 40, n. 9, p. 1361-1403, 1918.

LIMA, G. L. Desenvolvimento e aplicação de bio-adsorventes e catalisadores magnéticos derivados de resíduos de biomassa. 2018. Tese (Doutorado) – Universidade Federal da Bahia. Instituto de Química, Salvador, 2018.

LOPES, Osmando F. et al. Óxidos de nióbio: uma visão sobre a síntese do Nb2O5 e sua aplicação em fotocatálise heterogênea. *Química Nova*, v. 38, n. 1, p. 106-117, 2015.

MASSARANI, G. Fluidodinâmica em Sistemas Particulados. Rio de Janeiro: Editora UFRJ, 1997.
Ministério de Minas e Energia, Brasil, 2024.

MORAIS, Lidiane Alves de. Síntese, caracterização e estudo das propriedades fotocatalíticas de compostos de nióbio em matrizes ambientais. 2016.

NG, J. C. Y.; CHEUNG, W. H.; McKay, G. Equilibrium studies of the sorption of Cu(II) ions onto chitosan. *Journal of Colloid and Interface Science*, v. 255, p. 64-74, 2002.

NASCIMENTO, R. F. do et al. Adsorção: aspectos teóricos e aplicações ambientais. Fortaleza: Imprensa Universitária, 2014. 256 p.

OTAVO-LOAIZA, Ronald A.; SANABRIA-GONZÁLEZ, Nancy R.; GIRALDO-GÓMEZ, Gloria I. Tartrazine Removal from Aqueous Solution by HDTMA-Br-Modified Colombian Bentonite. *The Scientific World Journal*, v. 2019, n. 1, p. 2042563, 2019.

PAPAGIANNAKI, Dimitra et al. From monitoring to treatment, how to improve water quality: The pharmaceuticals case. *Chemical Engineering Journal Advances*, v. 10, p. 100245, 2022.

ROSÁRIO, Adriane Viana do. Investigação da formação da fase óxido e estudo da influência da microestrutura e morfologia nas propriedades eletrocrômicas de filmes finos de Nb2O5. 2002.
SILVA, M. V. C. O. Niobium oxide (V): characterization study and evaluation of photocatalytic properties. Master Thesis, 2022.

SKOOG, D. A.; WEST, D. M.; HOLLER, F. J.; CROUCH, S. R. *Thomson Learning*. 8. ed., 2007.

TAHER, Tarmizi et al. Adsorptive removal and photocatalytic decomposition of cationic dyes on niobium oxide with deformed orthorhombic structure. *Journal of Hazardous Materials*, v. 415, p. 125635, 2021.